Theoretical study of the formation, evolution, and breaking of gold nanowires

E. Z. da Silva*
Instituto de Física "Gleb Wataghin," UNICAMP, CP 6165, 13083-970, Campinas, SP, Brazil

Frederico D. Novaes, Antônio J. R. da Silva,† and A. Fazzio‡
Instituto de Física, Universidade de São Paulo, CP 66318, 05315-970, São Paulo, SP, Brazil
(Received 7 August 2003; published 17 March 2004)

Real time imaging experiments with metal nanowires (NWs), in particular gold under stress, that show their formation, evolution, and breaking, were obtained with high resolution electron microscopy. In order to understand these results, we use density functional theory (DFT) based methods to simulate the evolution of Au NWs. First we use a tight-binding molecular dynamics (TBMD) method to understand the mechanisms of formation of very thin gold NWs. We present realistic simulations for the breaking of these NWs, whose main features are very similar to the experimental results. We show how defects lead to the formation of one-atom constrictions in the Au NW, which evolves into a one-atom-thick necklace chain. Similarly to the experimental results, we obtain that these necklaces can get as long as five-atoms from apex to apex. Before breaking, we obtain relatively large Au-Au bond distances, of the order of 3.0–3.1 Å. A further pull of the wire causes a sudden increase of one of the bond distances, indicating the breaking of the NW. To get some more insight into the electronic structure aspects of this problem, we considered several of our tight-binding structures before breaking and studied them in detail using an *ab initio* method based on the DFT. By pulling the wire quasistatically in this case, we also observed the breaking of the wire at similar distances as in the TBMD. This result was independent of the exchange-correlation potential used—either the local density approximation (LDA) or the generalized gradient approximation (GGA). The pulling force before rupture was obtained as 2.4 nN for the LDA, and 1.9 nN for the GGA. Finally, we also present a detailed analysis of the electronic structure properties for the Au neck atoms, such as the density of states and charge densities, for some configurations before the rupture.

DOI: 10.1103/PhysRevB.69.115411 PACS number(s): 68.65.−k, 71.15.Pd, 68.37.Lp

I. INTRODUCTION

Last century's final decade witnessed a revolution in terms of new and powerful experimental techniques,[1] such as scanning tunneling microscopy (STM), atomic force microscopy (AFM), and high resolution transmission electron microscopy (HRTEM). These new techniques revolutionized the understanding of matter at its atomic level, not only due to the fact that they permit to image atoms, but also because some of then allow atomic manipulation. As a consequence, nanoscience became a reality, and research in nanophysics is one of the important efforts nowadays. This research is interesting from the fundamental point of view of understanding basic physics, but it has also a great appeal because it can lead to devices with possibilities of offering new technological solutions, going beyond the present silicon based technology. This ability to manipulate matter at the atomic scale has brought nanoscience into the forefront of research, due to the possibilities of both immediate and long term technological applications. In the present microelectronics technology, electric contacts are very important parts of devices. In the nanotechnology world, whatever surprises it may bring in terms of new devices, electric contacts will probably continue to play an important role, and most likely will play an even more fundamental role. Therefore, the research of nanocontacts is of paramount importance for the development of components for the next generation of devices.

Among metals used for contacts, gold occupies a privileged position, due to its singular properties, such as malleability and low reactivity (bulk phase). Even though gold is a well known bulk material, many surprises appear when one moves to low-dimensional structures. For example, the transition from crystalline (fcc) gold to nanowires presents an interesting organization of matter, a subject not yet fully understood.[2] Au nanowires have been experimentally produced by different techniques;[3] the first report of their fabrication was by contacting a STM tip with a metal surface.[4] Since then, similar approaches have been used by many groups.[5–8] The technique of ''break'' junctions, originally introduced to study thin wire superconductors,[9] was extended and became the mechanically controllable break junction, introduced by Muller *et al.*,[10] which has also been used extensively to study nanowires. Moreover, imaging techniques, such as HRTEM,[11] have also been employed extensively in the study of nanowires. Ohnishi *et al.*[7] developed a STM experiment inside a HRTEM chamber, and measured conductance with simultaneous images of Au nanowires. In this way, for the first time, it was shown that one-atom thick wires were indeed formed under tensile stress, and displayed one quantum of conductance. This same group also developed a way of producing nanowires from self-supported thin films, which have been used in real time imaging experiments of metal nanowires.[11–14] This technique, initially developed by Kondo and Takayanagi,[11] is an experimental procedure that produces stable Au NWs through electron-beam irradiation of a Au thin film in a ultrahigh vacuum transmission electron microscope. Nanoholes are produced in Au (001) films, with a $\simeq 3$-nm thickness, by this electron beam

bombardment. In this way, free standing nanobridges were produced, which, upon further irradiation, became thinner. The electron beam was then turned into an observation mode (HRTEM), which allowed a combination of atomic resolution with real time image acquisition, therefore, permitting the real time observation of the nanowire's (NW's) dynamical evolution. One important finding of these studies was that, under stress, these wires, before breaking, can get as thin as one-atom chains, and as long as five suspended atoms, with unexpected quite large interatomic distances of $\simeq 3.6$ Å between the chain atoms.[7,13,14] Some recent works,[15–18] however, have proposed that impurities might be the cause of such large distances. Other surprises, such as helical nanowire structures, have been theoretically predicted,[19] for Pb and Al, and experimentally observed[12] in gold.

One of the important reasons to understand these nanowires is that, between two of the tips of very thin NWs, it is possible to insert small structures, such as carbon buckyballs,[20] or small organic molecules,[21] with the possibility of use as devices. Calculations to understand such systems have been done.[22,23] A recent calculation of organic molecules attached to a Au surface, and then pulled out of the surface, has shown that the molecular structure is transformed into a composite system, namely, a molecule attached to a Au nanowire pulled out of the Au surface. In other words, the molecule instead of breaking when pulled out of the surface, draws out from it a one-atom-thick nanowire that is stretched similarly to the ones that we simulate here. It is this nanowire that eventually breaks, letting the molecule free from this surface.[24]

Parallel to these developments in nanotechnology, that made it possible to manipulate and design smaller interesting structures almost every day, computer simulations, with new methodologies and the increasing power of state-of-the-art computers, are also able to test and even propose new structures, the so-called computer assisted virtual projects of new structures. Along the lines of the present discussion of metal NWs, predictions have been made. Mostly using molecular dynamics with classical many body potentials, many simulations of experimental setups, and also many new proposed structures, were presented.[2,25,26] The first works in this area started in an attempt to understand the wetting process that occurred with Au STM tips, when in contact with a Au surface.[27] Simulations with classical potentials for NWs were performed in order to understand the experiments. As mentioned previously, Gulseren, Ercolessi, and Tosatti[19] predicted, based on computer simulations with classical potentials, that Al and Pb thin wires would ''prefer'' to have what they called ''weird'' structures, as opposed to the expected crystalline multifaceted structures. This type of approach to the problem considers the structural question of competition between internal packing and minimal surface energy. Albeit important, these studies should be complemented and confirmed by *ab initio* studies. Unfortunately, *ab initio* studies are very demanding computationally, and very few studies were done so far. One step towards this goal is to consider tight-binding parametrizations for the underlying electronic structure, in a molecular dynamics formulation of the problem [tight-binding molecular dynamics (TBMD)], therefore taking into account, explicitly, the effect of the electrons in the problem. A recent tight-binding scheme, proposed by Mehl and Papaconstantopoulos,[28–30] provided a method that permits calculations to regimes involving 10^2–10^3 atoms in the unit cell, and also for relatively long simulation times at finite temperatures, expanding the simulations to a range beyond the present capabilities of *ab initio* calculations. More recently, the NRL group has developed a new TBMD scheme that has been successful in treating many properties of metals.[29–31]

The structure of this paper is as follows. In Sec. II, after this general introduction, we describe the methods used in the present calculations. We first describe the TBMD method, followed by a presentation of the *ab initio* method that we have used to study the electronic structure of these nanowires, generated through the TBMD procedure. In Sec. III we discuss the results of the present calculations. We first present the TBMD simulations, which allow us to understand the formation mechanisms of these atomically thin Au nanowires. We study in detail the evolution of Au nanowires under stress, and show how defects induce the formation of necks that eventually will form the one-atom chains. These chains, due to stress, grow up to a point where they break. We then present density function theory calculations of selected stages of the molecular dynamics (MD) evolution, which were used both to validate the accuracy of the TBMD simulations as well as to discuss the electronic structure of these nanowires. Finally, in Sec. IV we give conclusions and perspectives opened up by this work.

II. METHODS

Density Functional Theory (DFT) is the basis for electronic structure calculations, and we use two methods to study nanowires, both based on DFT. First we study the formation, dynamical evolution and the breaking of nanowires using the DFT derived tight-binding molecular dynamics method. We then perform *ab initio* calculations for selected configurations from the TBMD simulations, and study their electronic structure properties, and the nanowire's breaking process.

A. Tight-binding molecular dynamics

As discussed above, we initially performed TBMD simulations.[28–30] This method lies in between first principles and empirical methods: it is more accurate than empirical potential methods because it explicitly includes the electronic structure, and is much faster than first principles methods. The electronic structure of gold is described using a tight-binding fit developed by Mehl and Papaconstantopoulos,[28] and a brief description of their procedure is presented here. The parameters used[29] were fitted to reproduce *ab initio* density functional theory calculations of band structures and total energies as a function of volume for fcc, bcc, and simple-cubic (sc) structures. The data base includes ten fcc, six bcc, and five sc structures. Energies at very small volumes (60% of the local equilibrium volume) were included. In Ref. 31 Kirchhoff *et al.* show that the

tight-binding parametrizations for static properties like bulk modulus, elastic constants, and phonon frequencies are in good agreement with experiments (errors between 2% and 10%), and also that the use of these TB parameters in MD simulations gave a temperature dependence of lattice constant and atomic mean-square displacements also in good agreement with experiments (errors of the order of 1%). Also, for liquid gold at $T=1773$ K, the calculated radial distribution function showed good agreement with the experimental values. In conclusion, the use of this parametrization for bulk solid and liquid gold gave very good results.[31] This parametrization can be obtained at their web site.[29]

Since this TBMD has been successfully used[31] to study crystalline and liquid Au, we have used it to study Au nanowires. The MD procedure uses the NRL-TB parametrization[28,29] for the electronic states. The electronic structure is calculated using a diagonalization procedure. The equations of motion are integrated using the Verlet algorithm and the time step used was $\Delta t=1$ fs. To perform the annealing, we have used a friction parameter $\gamma=0.001$ fs^{-1}. Brillouin zone sampling was done using the Γ point. The periodic supercells used in all calculations had dimensions (20 Å, 20 Å, L_W).

The dynamical evolution of the wire under stress is simulated in the following way: (i) Simulations start from a stack of ten planes of seven atoms, oriented along the (111) growth direction. The initial periodic super-cell has $L_W=24.0$ Å along the tube direction, which corresponds to an elongation of 0.4 Å (or $\sim 2\%$) when compared to an ideal stack of ten (111) planes in bulk Au. This initial configuration is warmed to 600 K, and then annealed to lower temperatures, resulting in a cylindrical final geometry with the surface atoms reconstructing into a densely packed structure. (ii) The wire is elongated by 0.5 Å. (iii) The temperature is increased to 400 K. (iv) The system is annealed for 4000 MD steps (4 ps) up to a temperature of approximately 30 K. Steps (ii)–(iv) are repeated until we observe the rupture of the wire. Even though this protocol corresponds to elongation rates much higher than the experimental ones (but similar to all other rates used in atomistic simulations), it leads to forces that are quite similar to the measured values[32,33] (see below). Moreover, the time interval between each elongation step is much larger than a typical relaxation time for gold. Finally, it is worth mentioning that all the general features discussed below were also present in other simulations where we varied either the cell elongation (step ii above) or the simulation temperature [step (iii) above]. In fact we describe here a second simulation performed with the same procedure with the only difference that in step iii the temperature was raised to 300 K.

B. First principles calculations

The simulations using TBMD gave very good insights into the mechanisms of formation and also the breaking of Au nanowires; nevertheless one question remained unanswered: how different would these be from an *ab initio* calculation? We therefore performed DFT calculation for selected structures from the TBMD simulations. All our results are based on *ab initio* total energy DFT (Ref. 34) calculations using numerical orbitals as basis sets.

TABLE I. Calculated binding energies and forces for Au_2 for different approximations.

DFT	Base	E_S (eV)	Mesh (Ry)	E_B (eV)	Force (nN)
LDA	DZP	0.07	250	2.99	3.52
GGA	DZP	0.07	250	2.38	2.95
Expt.				2.3	

We have used the SIESTA code,[35] which performs fully self-consistent calculations solving the Kohn-Sham equations. The interaction between the valence electrons and ionic cores are described through standard norm-conserving Troullier-Martins pseudopotentials.[36] We use periodic-boundary conditions and a supercell approximation with a lateral separation of 20 Å between wires to make sure that they do not interact with each other. We have used the X point for the Brillouin zone sampling, though tests with eight Monkhorst-Pack **k** points[37] along the tube axis were also performed. After each change in the wire's length, the positions of all the atoms in the supercell were relaxed until all the force components were smaller than 0.03 eV/Å. There are some crucial approximations that have to be tested carefully in order to have a reliable result with the SIESTA code. First of all, the quality of the basis set, in terms of how many functions are used to describe each angular momentum channel, is crucial. To obtain good results it is necessary to use a double-zeta basis set. However, it is also important to check if it is necessary to include a polarization function. The second parameter to be considered is the range of the basis function, which is characterized by a confining energy, usually called the energy shift.[38] Another critical approximation is the energy cutoff, which defines the grid used to represent the charge density. Finally, a very important approximation at the level of DFT is the exchange-correlation functional. We performed calculations both at the local density approximation (LDA) and the generalized gradient approximation (GGA).[39] From a series of tests for both bulk gold and a gold dimmer, we have concluded that a good description is given by a split-valence double-zeta basis set with polarization function with a confining energy shift of 0.07 eV,[38] and a cutoff of 250 Ry for the grid integration. In Table I we present results for the Au_2 for the LDA and GGA approximation. As can be seen, the GGA approximation gives a much better value for the binding energy, and a smaller value for maximum force required to separate the gold atoms. For the present discussion of the nanowires, we have also performed calculations using the GGA and LDA approximations to examine the wire's rupture (see below). Similarly to the dimer results, our calculations show that the GGA breaking forces are smaller than LDA ones, and in better agreement with the experimental results (for the LDA, we have obtained 2.4 nN, for the GGA we have obtained 1.9 nN, and the experimental result[33] is 1.5 ± 0.3 nN). It should be mentioned that, even though the GGA equilibrium distances tend

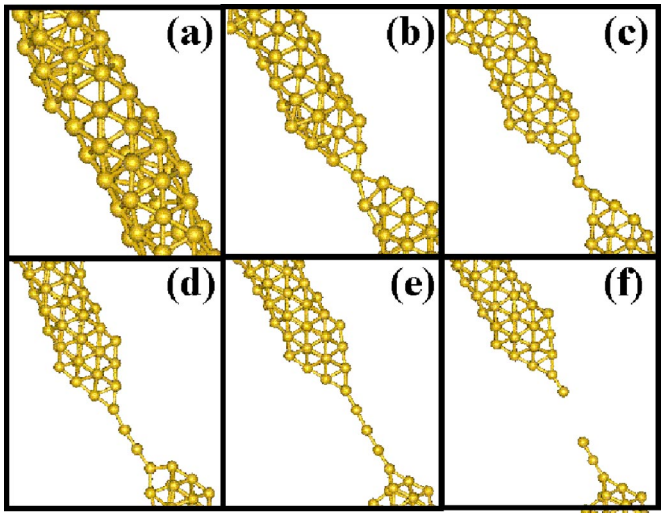

FIG. 1. Atomic configurations of a gold nanowire at selected elongation stages (simulation I), obtained through tight-binding molecular dynamics simulations. The configurations presented correspond to the following wire lengths: (a) 25.5 Å, (b) 33.0 Å, (c) 35.0 Å, (d) 38.0 Å, (e) 40.5 Å, and (f) 43.0 Å.

to be larger than the LDA ones, the maximum Au-Au rupture distances are very similar in both cases, indicating that the differences between the GGA and LDA geometrical parameters for the equilibrium structures do not reflect their behavior under stress.

III. RESULTS

A. TBMD—dynamical evolution

Many simulations were performed and in the present paper we discuss two of these simulations and they will be referred in the text as simulations I and II. To study the evolution of gold nanowires under stress, we considered a set of ten planes of seven atoms each, oriented initially along the (111) growth direction. The periodic supercell had an initial length $L_W = 24.0$ Å along the tube direction. After one thermalization cycle, as described above in the Sec. II, the initial configuration attained a cylindrical final geometry with the external atoms reconstructing into a densely packed structure. After this thermalization procedure, we repeated cycles where the wire was elongated by 0.5 Å, the temperature was increased to 400 K in simulation I and to 300 K in simulation II , and the system was annealed for 4000 MD steps (4 ps) until a temperature of approximately 30 K was reached. This cycle was repeated until the rupture of the wires.

Simulation I is discussed using six selected snapshots of the evolution of the wire displayed in Fig. 1. As can be seen from Fig. 1(a), the wire tends to become hollow as it is pulled, which is caused by the motion of atoms from the center of the wire towards its surface. As a consequence, the seven-atom planes are transformed into six-atom rings, stacked along the tube axis, as can be seen in Fig. 1(a) ($L_W = 25.5$ Å). In this configuration, the Au atoms form a tube which is essentially a folded (111) sheet, similar to what happens in carbon nanotubes.[40] Experiments reporting hollow Au nanowires were presented by Kondo *et al.*,[12] where a hollow six-atom ring was covered by another sheet of Au atoms consisting of a 13-atom ring. Hollow nanowires, with six-atom rings, were reported recently in Pt nanowires.[41] This is consistent with the fact that the Au atoms always try to expose a closepacked surface. We observe that a new ring of six atoms is inserted when the increase in the length of the wire is of the order of the (111) interplanar distance in bulk Au (~ 2.3 Å). When the rings are somewhat compressed, we observe a small helicity along the tube axis. This probably happens in order to accommodate the atoms, and the helicity decreases as the wire is pulled.

The evolution from the hollow tube of Fig. 1(a) to the one atom constriction in Fig. 1(b) occurs due to a very interesting mechanism of defect formation that was first discussed by da Silva *et al.*[26] Further evolution with the inclusion of more atoms to the chain is due to a competition between elastic forces and atomic displacements. At one side the elastic forces grow and if the tips are not very symmetrical, atoms move to relax these forces.[32] When the tip becomes very symmetrical, the wire withholds the forces up to a critical breaking value when rupture occurs.

The development of an one-atom neck displayed in Fig. 1(b), occurs when $L_W = 33$ Å. Forces in the interval from elongations of $L_W = 31-34$ Å show a buildup from 1.2 up to 2.6 nN, right before the formation of the one-atom neck, followed by a sudden force reduction to a value of 1.3 nN with the atomic rearrangement. This sawtooth behavior is similar to experimental results.[32,33]

In general terms, the thinning down process is due to a defect structure that leads to the one atom constriction shown in Fig. 1(b).[26] The process is accomplished by surface atoms drifting to the tips as thermodynamics would indicate, as pointed out by Torres *et al.*[42] Once the one-atom constriction that separates the two tips is formed, a new process is initiated. Atoms from only one of the tips start to move to the neck, and are incorporated into the one-dimensional chain that grows as long as five atoms from apex to apex, with three suspended atoms. The details of the neck formation are presented in Fig. 2. A defect structure, shown in Fig. 2(a), is responsible for the development of the neck. This defect structure is composed of two interstitial atoms (marked in a different color in Fig. 2(a), close to the axis of the wire) near a six-atom ring [also in a different color in Fig. 2(a)], plus an external atom [again, marked in a different color in Fig. 2(a)]. These defect atoms [Fig. 2(b)—the relevant defect atoms will always be highlighted in Figs. 2(b)–2(g)] rearrange themselves into a four-atom ring plus a five-atom ring [Fig. 2(c)]. The five-atom ring, being more unstable than the four-atom one, further evolves into a two-atom and a three-atom structure [Fig. 2(d)]. A structure similar to a two-dimensional ladder develops [Fig. 2(e)], finally forming the one-atom constriction of Fig. 1(b), which is also shown in detail in Fig. 2(f). The one-atom constriction starts to grow, forming a one-dimensional wire, incorporating more atoms into the one-atom-thick necklace, as can be seen from Figs. 1(c)–1(e). This one-atom chain shows an apex lateral movement, during its dynamical evolution, similarly to the experiments.[14] Finally, the breaking of the nanowire occurs

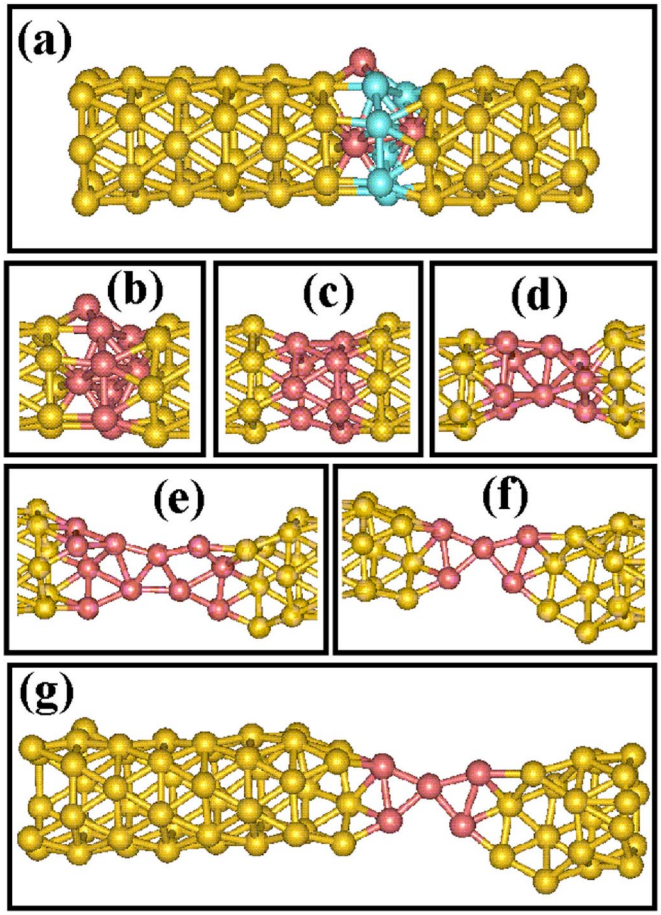

FIG. 2. Atomic configurations of a gold nanowire at selected elongation stages where the dynamical evolution of the one-atom constriction is detailed (simulation I). It shows the defect structure responsible for the neck formation, and its evolution, from $L_W = 27.0–33.0$ Å. The configuration in (a) shows the defect structure (highlighted in a different color): two interstitial and one external Au atoms surrounding a six-Au-atom ring. The evolution of this defect structure (b) is depicted from frame (c) to frame (g). This final frame corresponds to the one-atom neck displayed in Fig. 1(b) (the relevant defect atoms are always marked by a different color).

when, at $L_W = 41.0$ Å [Fig. 1(f)], there is a sudden increase of one of the bond distances from a value of ~ 3.1 Å to a value close to 4.3 Å. Further pull of the wire simply increases this distance. It is worth mentioning that when the necklace breaks, the atomic structure of the unstable tip is similar to the other one. Therefore, it can be said that the wire will only break after the tips attain a rather stable structure. Before this configuration is reached, the system prefers to move the atoms from the less stable positions in the tip towards the neck, rather than breaking the wire. This behavior is similar to what has been recently reported by Rubio-Bollinger *et al.*[33]

Simulation II is discussed using six selected snapshots of the evolution of the wire displayed in Fig. 3. As can be seen from Fig. 3(a) ($L_W = 26.0$ Å), the wire tends to become hollow as it is pulled, which is caused by the motion of atoms from the center of the wire towards its surface, similarly to the evolution of the previous simulation, showing that this is

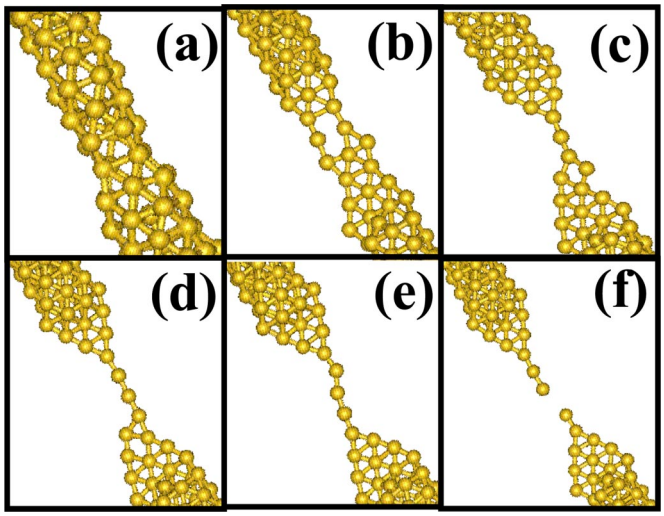

FIG. 3. Atomic configurations of a gold nanowire at selected elongation stages (simulation II), obtained through tight-binding molecular dynamics simulations. The configurations presented correspond to the following wire lengths: (a) 26.0 Å, (b) 36.5 Å, (c) 38.0 Å, (d) 40.0 Å, (e) 40.5 Å, and (f) 43.5 Å.

a general feature of this type of evolution. As a consequence, the seven-atom planes are transformed into six-atom rings, stacked along the tube axis, as can be seen in Fig. 3(a). In Fig. 3(a) one can see a narrow section with a four-atom ring. A distortion leading to the narrowing of the wire develops at this point. As the wire is pulled a planar four-atom structure develops connecting the two wire leads. The rearrangements that occur in the evolution leading to the structure of frame 3(c) are detailed in Fig. 4. The result is the formation of a narrow constriction with one suspended atom attached to two Au atoms from the two leads. Figure 3(d) shows the incorporation of a second suspended atom. Figure 3(e) shows the third atom incorporated and also displays the one-atom wire sideway movements, as the wire grows with incorporation of more atoms. Figure 3(f) shows the wire just after its breaking.

The evolution of the wire in Fig. 3, from frames (b) to (c) is displayed in detailed form in Fig. 4. In Fig. 4(a) the atoms responsible for the rearrangements are marked in different colors, and their evolution can be followed. Two of them are attached from the left, to two other atoms that make the side of a stable hexagon. As the stress builds up, it is released by rearrangements of these three atoms that are not in symmetrical positions. First the one on the right rearranges to become the right tip [Fig. 4(c)]. The top defect atom moves in order to become the tip of the left lead [Fig. 4(c)]. Therefore, these two atoms move to become the tips of the left and right leads, respectively, whereas the third atom is the one that stays suspended connecting the two leads as seen in Fig. 4(e) and also Fig. 3(c). When we compare the neck formation in simulations I and II we note some general features: (1) In both cases, the constriction started to form in a region where there were two defective rings, one with five and one with four atoms. (2) The subsequent evolution of the wire from this point on were not exactly the same; however, both were

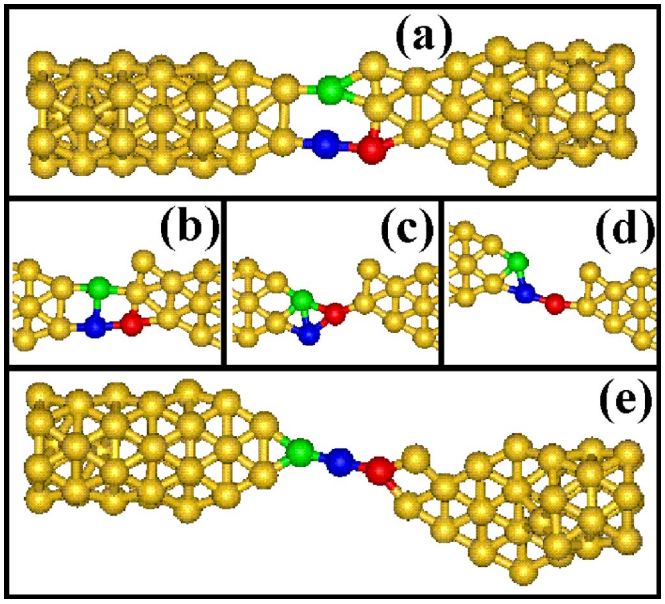

FIG. 4. Atomic configurations of a gold nanowire at selected elongation stages (simulation II), obtained through tight-binding molecular dynamics simulations. The dynamical evolution of the one-atom constriction is detailed. It shows the defect structure responsible for the neck formation, and its evolution, from $L_W = 36.5–38.0$ Å. The configuration in (a) shows the defect structure from Fig. 3(b): the three atoms involved in the process are marked in different colors. The evolution of this defect structure can be followed in the sequence depicted from frame (b) to frame (e). This final frame corresponds to the one suspended atom neck displayed in Fig. 3(c).

dictated by the general trend of exposing (111) surfaces. (3) Once hexagonal-like structures are formed at the tip, they tend to be rather stable.

Prior to breaking, both simulations show rather symmetrical tips. They vary slightly, but in both cases they are terminations of (111) planes sharing atoms (Fig. 5). The tips can be viewed in two ways, either as clusters stacked along the wire's direction (Fig. 6) or also as a merger of two pieces of (111) sheets (two hexagonal structures), represented by the

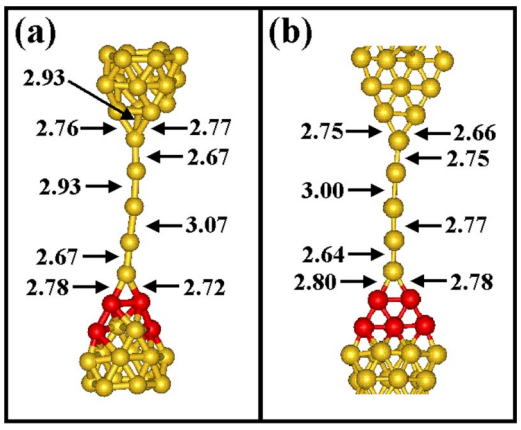

FIG. 5. Structures of the nanowires just before breaking, showing the details of the one-atom-thick necklace. (a) Simulation I. (b) Simulation II. All the bond distances are in Å.

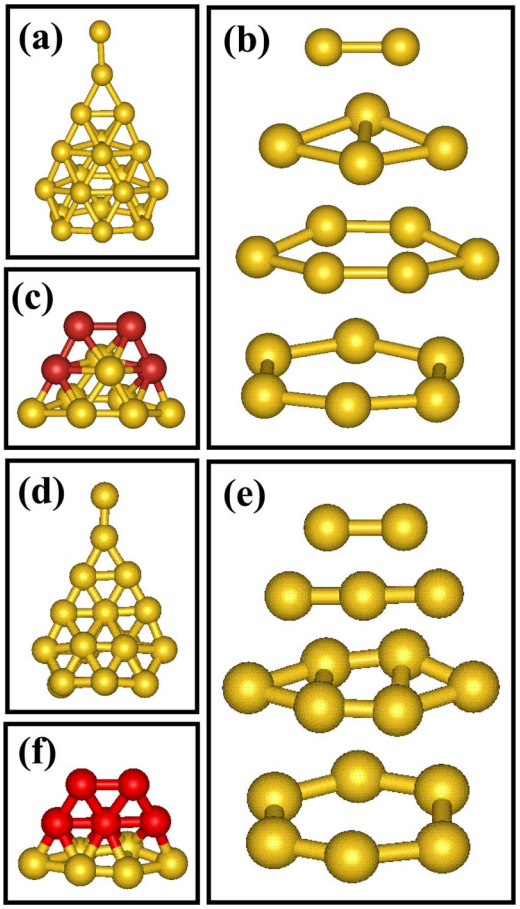

FIG. 6. Stability of the nanowire tips. The tips, before and after breaking, show highly symmetric and stable structures [(a), (b), and (c) refer to simulation I and (d), (e), and (f) refer to simulation II]. In (a) and (d) the whole tips are shown, whereas in (b) and (e) the cluster layers forming them are presented. Finally, in (c) and (f) a French-hat-like structure is shown.

colored atoms in Figs. 5 and 6. Figure 5 displays the structure of wires of simulations I [Fig. 5(a)] and II [Fig. 5(b)]. In both cases, the one atom thick wires evolve to a structure as long as five atoms. The Au-Au distances get as long as 3.1 Å in both simulations, distances much shorter than some of the observed experimental values.[11,14] As we will show in the discussion of *ab initio* calculations repeated for these wires, all calculations with pure Au atoms fail to give longer Au-Au bonds.

One can further understand the stability of the Au tips with the aid of Fig. 6, where the tips from simulation I [Figs. 6(a)–6(c)] and simulation II [Figs. 6(d)–6(f)] are shown. Figures 6(a) and 6(d) show the tips of the two structures prior to the breaking of the wires. Figures 6(b) and 6(e) present exploded views along the Au wire direction, showing how the tips are formed out of rather stable Au clusters that are nicely stacked on top of each other. From the thick portion of the tip and moving towards its end, both tips start with a symmetrical six-atom ring, very similar to the others that make the wire. On top of it there is a rotated six-atom ring, which distorts in order to accommodate either a four-atom kite-type structure, as occurs in simulation I, or a three

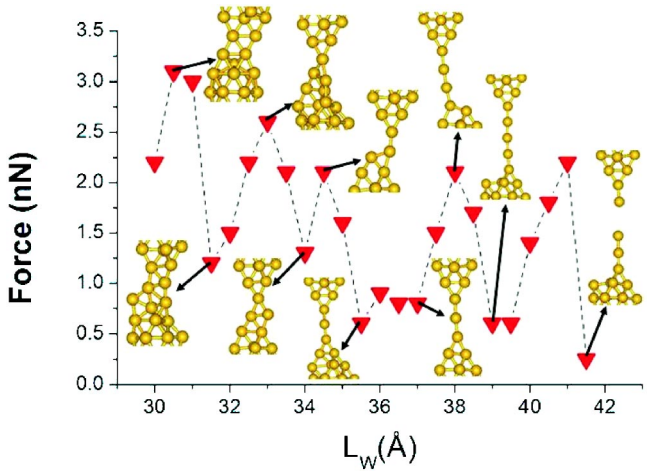

FIG. 7. Calculated pulling force acting on the Au nanowire for selected stages of simulation I. Arrows with associated configurations correspond to major structural rearrangements of the wire.

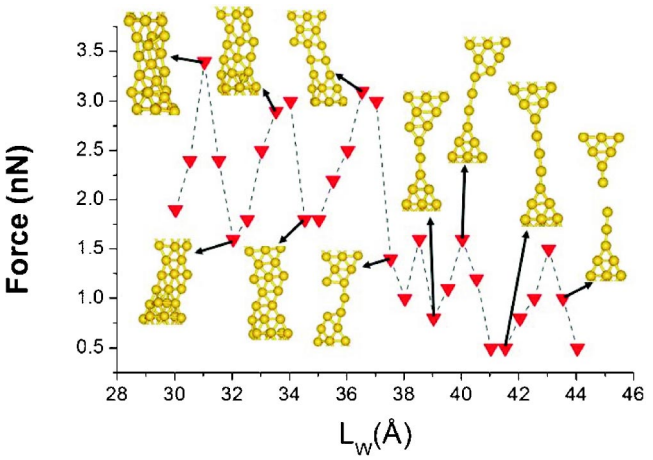

FIG. 8. Calculated pulling force acting on the Au nanowire for selected stages of simulation II. Arrows with associated configurations correspond to major structural rearrangements of the wire.

atom line, as in simulation II. Finally, a dimer terminates both tips, which is the place where the one-atom chain is attached. In Figs. 6(c) and 6(f) the whole tip structures are displayed, where colored atoms are the ones shared by the two terminating (111)-like planes. In Fig. 6(c), four atoms join two hexagons terminating the tip for simulation I, whereas in Fig. 6(e) the trimer and dimer discussed above [Fig. 6(e)] are shared by the two (111)-like planes, closing the tip as ''melted'' hexagons. The two tips are very symmetrical and rather similar, both sharing atoms at the termination point in order to end the wire with (111)-like planes.

One of the interesting aspects of the evolution of these nanowires can be observed by an analysis of the applied forces. From the total energies of the final configuration of each elongation stage, these forces were estimated. Similar to recent studies of mechanical properties associated with the formation mechanisms of atomically thin Au nanowires,[33] we observe that the dynamical evolution of the nanowires correspond to elastic stages followed by sudden structural relaxations, which are reflected in a sawtooth behavior of the pulling force acting on the wires, as can be seen[32] in Fig. 7 for simulation I, and in Fig. 8 for simulation II. From the insets in these figures, it can be seen that the elastic stages correspond to the building up of stress mostly due to the increase of the interatomic distances. The force relaxations, on the other hand, correspond to either concerted rearrangements of the atoms, mainly at the defective part of the wire, as previously depicted in Fig. 2 for simulation I and Fig. 4 for simulation II, or to the insertion of a new atom into the chain, after the one-atom constrictions were formed. We obtain a value for the applied force right before the breaking of the nanowire around 2.2 nN for simulation I, and 1.5 nN for simulation II. These results are in good agreement with the experimental value[33] of 1.5 ± 0.3 nN.

B. DFT—breaking wires using first principles

Nanowires are extremely different from bulk metals, and in particular for one atom thick wires, the coordination of Au atoms is so small (two neighbors) that MD with effective potentials, like Gupta type potentials fitted to bulk properties, are not reliable. For this reason, we have used the much more accurate TB formulation, as described in Sec. II in great detail. However, as the TB is also fitted to reproduce bulk properties, it would be highly desirable to compare the TB results with fully *ab initio* calculations. We have, therefore, performed *ab initio* DFT calculations, as described above, for some structures obtained from the TB simulation I. In Fig. 9(a) we show the TB configuration for $L_W = 40.5$ Å an elongation 0.5 Å shorter than the critical breaking size. This

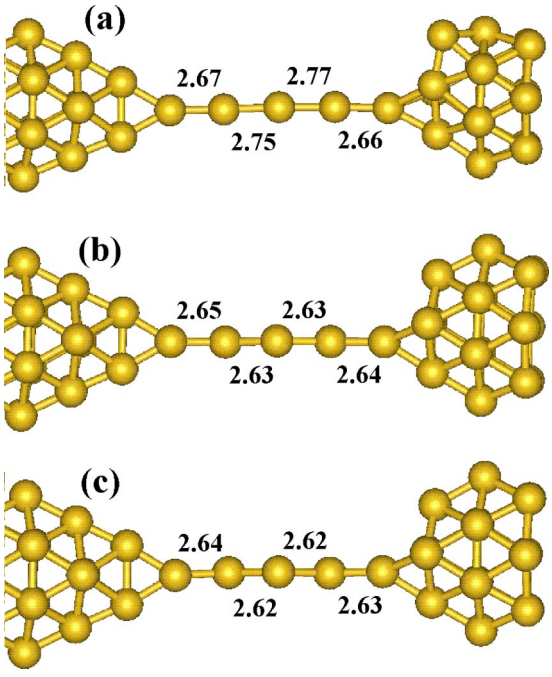

FIG. 9. Nanowire at $L_W = 40.5$ Å. Structure (a) is from the TBMD simulation. Structure (b) is the same structure after an *ab initio* relaxation of the forces using the LDA. Structure (c) The same structure after an *ab initio* relaxation of the forces using GGA. All displayed distances in Å.

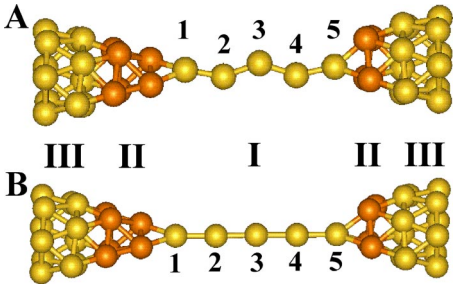

FIG. 10. Final stages of evolution and breaking of a nanowire using *ab initio* calculations. Structure A is from the TBMD simulation after *ab initio* relaxation of the forces using SIESTA. Structure B is obtained prior to breaking using SIESTA (distances are given in Table II). The nanowire was considered as having three different types of atoms; I, single atom neck; II, tips; III, bulk wire. Atoms at the neck are labeled 1–5.

structure was fully relaxed using the *ab initio* methods described above, both at the LDA [Fig. 9(b)] and GGA [Fig. 9(c)] levels. As can be seen from Fig. 9, the overall structure is very similar in all cases, with very slight changes in the bond lengths at the *ab initio* level (the bond lengths are very similar for the GGA and LDA calculations) when compared to the TB result.

Besides this confirmation that the nanowire structural properties, prior to the rupture, are well described at the TB level, it is fundamental to make sure that the breaking is also being well described. Thus, the structures from Fig. 9 were pulled (by increasing the size of the supercell along the wire's length) all the way up to their ruptures, with the forces being relaxed at each elongation. For both the LDA and GGA calculations, the breaking of the wire occurred with similar bond distances as in the TBMD. This gave us confidence in the good parametrization of the TBMD. As mentioned above, the required forces to break the nanowires, right before their rupture, was 2.4 nN for the LDA and 1.9 nN for the GGA. The corresponding value at the TB level (simulation I) was 2.2 nN. The fact that this result is similar to the LDA value is consistent with the TB parametrization. The experimental result[33] for this force is 1.5 ± 0.3 nN. Since both the LDA and GGA calculations give very similar structural properties at the rupture point, but the GGA gives a better value for the force, when compared to the experimental result, further analysis will be presented only for the GGA approximation. These results are in good agreement with previous calculations of the breaking forces. Sánchez-Portal *et al.*[44] report a value of 2.2 nN for a LDA calculation, whereas Rubio-Bollinger *et al.*[33] report various calculations at the GGA level, and obtain values between 1.6 and 1.7 nN. They mention, however, that the final results depend on the exchange-correlation functional used in the calculations: when they used the RPBE approximation[45] they obtained a force of 1.4 nN. Ribeiro and Cohen[46] obtained recently, using a LDA approximation, a value of 2.5 nN. Finally, Kruger *et al.*[24] obtained a force of 1.4 nN when breaking a wire produced by pulling an organic molecules attached to a Au surface.

In Fig. 10 we present the same structure from Fig. 9(c) (called structure A from now on), but from a different perspective. As can be seen, the gold atoms at the neck form a zigzag configuration, as has been reported previously by other groups.[44] In Fig. 10 we also show the structure prior to breaking (called structure B from now on), and as can be seen, the zigzag configuration is not present anymore. The distances between the neck Au atoms, which are labeled from 1 to 5 in Fig. 10, are presented in Table II. As can be seen, the Au-Au distances right before the wire's rupture are all similar (between 2.9 and 3.0 Å). Moreover, the maximum distance obtained in this case was $\simeq 3.0$ Å. This result is similar to what we have obtained before in our TB simulation I,[26] as discussed in Sec. II, and similar to other theoretical results.[42] This is in good agreement with both the results of Takai *et al.*[43] and the position of the first peak in the histogram of Au-Au distances in Ref. 15. Besides the DFT calculations using localized basis set (SIESTA code), we have also performed some calculations using a plane wave (PW) basis set (we have performed *ab initio* calculations, based on the DFT within the GGA approximation,[47] with ultrasoft pseudopotentials[48] and a plane wave expansion up to 180 eV, as implemented in the VASP code.[49] All other approximations were the same as in the SIESTA calculations). The Au-Au distances for the neck atoms obtained in this latter case, also prior to the rupture, are shown in Table II. As can be seen, the distances are somewhat smaller than in the localized basis set calculation, except for the Au-Au bond that broke, which had a maximum distance of approximately 3.1 Å. All these results strongly indicate that, in pure Au nanowires under tension, the limit for the Au-Au breaking distance is somewhere around 3.0–3.1 Å. Finally, in Table II we also compare the breaking force for the PW and localized basis set calculations, and see that the PW result is smaller, and closer to the experimental value. This suggests that, in order to have a very precise quantitative agreement, a well converged PW approach is recommended. However, the overall behavior is well described in both cases (and also in the TB calculations), specially the maximum distances.

TABLE II. Interatomic distances for atoms in the neck of structures of Fig. 10, and the breaking forces. PW is the same result as structure B (rupture) calculated with VASP.

Structure	(1,2)	(2,3)	(3,4)	(4,5)	F (nN)
A	2.64	2.62	2.62	2.63	
B	2.94	2.93	**2.96**	2.89	1.9
PW	2.75	**3.12**	2.75	2.85	1.4

In Fig. 11 we show contour plots for the total electronic charge density, in a plane that passes through all the neck atoms (region I of Fig. 10) of structure A. A metallic (delocalized) bonding character can be clearly seen, both along the neck atoms, as well as between the neck atoms and the tips, as inferred from the two inset figures in Fig. 11.

A similar analysis (Fig. 12) for the wire prior to its rupture (structure B), shows that the bonding character remains similar during the evolution of the wire. However, there is a clear decrease in the electronic density between the Au atoms, as expected. Even though it is not very clearcut, it is possible to

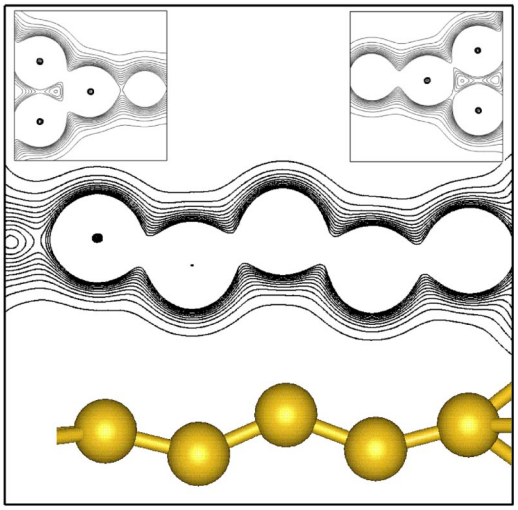

FIG. 11. Contour plots for region I of the wire (structure A) depicted in Fig. 10 (distances are given in Table II).

see from Fig. 12 that there is a decrease in the electronic density between the two Au atoms where the wire will break (atoms 3 and 4 of structure B in Fig. 10).

To gain a better insight into the electronic structures of the Au nanowires, in Figs. 13 and 14 we present projected density of states (DOS). In Fig. 13(a) we show the density of states for bulk Au, and in Figs. 13(b), 13(c), and 13(d) the DOS projected on the atoms of regions I, II and III, respectively, for both structures A and B (Fig. 10). As can be seen, the atoms in region III have an electronic structure already quite similar to the bulk. The somewhat small differences can be attributed to the different number of nearest neighbors. In fact, the projected DOS of Fig. 13 indicate that, as the number of nearest neighbors increases from region I to region III, there is an overall shift towards lower energies. While the tip DOS (regions II) are not very different from the bulk result, the neck atoms DOS (region I) are clearly distinct. They are much narrower, and located at higher energies. This is even more so prior to the wire's rupture, where one can see that the DOS becomes sharper, with a clear peak right below the Fermi energy.

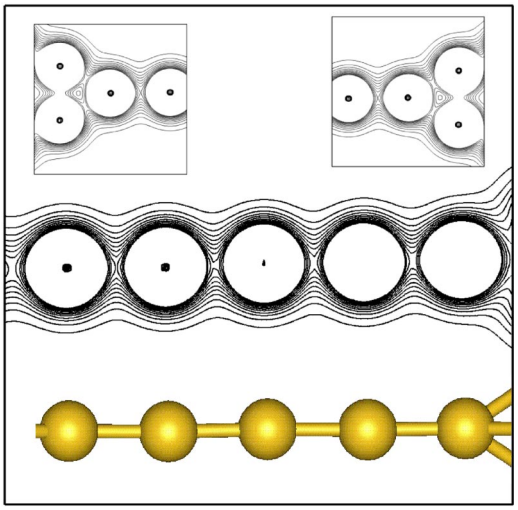

FIG. 12. Contour plots for region I of the wire (structure B) depicted in Fig. 11 (distances are given in Table II).

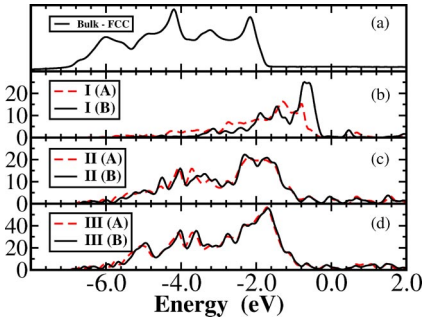

FIG. 13. Projected DOS for the two stages of evolution of the wire depicted in Fig. 12 [(A) relaxed structure, (B) structure prior to breaking] using *ab initio* calculations. (a) Bulk Au. (b) Contribution from atoms in region I. (c) Contribution from atoms in the region II (tip). (c) Contribution from atoms in region III ("bulklike").

In Fig. 14 we detail the projected DOS from region I, presenting the contribution of each neck atom (labeled 1–5 in Fig. 10). As can be seen once more, the coordination determines the peak positions. Atoms 2, 3, and 4, which have only two neighbors, have an overall shift of their projected DOS towards higher energies, when compared to atoms 1 and 5. Moreover, as atom 5 has four neighbors, whereas atom 1 has only three, its projected DOS is shifted towards lower energy values. As the wire is stretched towards its breaking length, the overlap between the Au atoms decreases as the Au-Au distances increase. This is reflected in the sharpening of the projected DOS of the neck atoms, but maintaining their relative energy positions, as above.

If we consider the contribution of atoms 2, 3, and 4 to the projected DOS at the Fermi level, we obtain 26% *s* character, 13% *p* character, and 61% *d* character for the initial configuration (structure A), whereas upon stretching these numbers change to 69%, 4%, and 26%, respectively (structure B). As can be seen, the character of the contribution to the DOS at the Fermi energy, for the neck atoms, shifts from a main *d* character to a stronger *s* contribution. For the DOS peak at $\simeq 0.5$ eV [Fig. 14(b) for structure B, right before rupture],

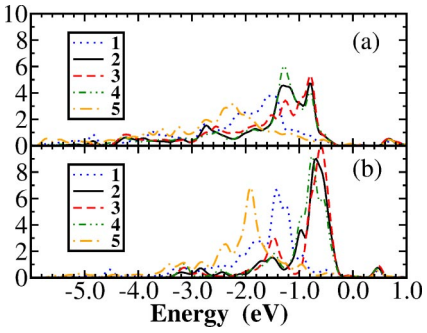

FIG. 14. Projected DOS for the five atoms in region I, corresponding to the one-dimensional neck, for the two stages of evolution of the wire depicted in Fig. 13 (a) presents the contributions of each atom for structure (A), and (b) presents the contributions of each atom structure (B).

the *s*, *p* and *d* contributions are 13%, 0%, and 87% (for atoms 2, 3, and 4), respectively, which indicated that this peak has a very strong d character.

IV. CONCLUSIONS AND PERSPECTIVES

This paper shows that TBMD simulations, in conjunction with first principles DFT calculations, can throw some light into the problem of formation, evolution and finally breaking of metallic nanowires. Our work has been focused on Au nanowires, but the procedures considered here can, and are, being used to study other nanowires. We have shown that the evolution of Au nanowires under stress are well described by the finite temperature TBMD simulation procedure. As a general feature of our simulations, the wires first reconstruct, with a migration of internal Au atoms of the wire towards the surface, producing single wall nanowires which are, basically, a (111) sheet folded into itself. The wires that emerge are stacks of six-atom rings, reproducing a single wall wire similar to the one proposed by Kondo and Takayangi[12] to explain their TEM images. The constrictions that eventually evolve to make the one-atom-thick wire start from defect structures that are formed during the dynamical evolution that leads to the formation of the single wall NWs. These defect structures become very thin, as thin as one atom constrictions connecting the two thicker tips. Due to further stress, the constriction starts to pull atoms from the thicker tips and incorporate them into the one-atom-thick wire, which is thus increased, getting as long as five atoms. This process continues and is a balance between elastic tensions and structural relaxations due to incorporation of atoms to release stress. The process of incorporating more atoms continues until the tips become very symmetrical and stable, then, as the tension grows to values larger than a critical force (experimentally determined to be $\simeq 1.5 \pm 0.3$ nN), the wire breaks. We have also shown that, starting with a structure from the TBMD simulation, at an elongation 0.5 Å before the breaking point, and using first principles calculations to study the evolution of the final stages of this wire, we obtained similar results to the TBMD. The wire breaks with Au-Au bonds at values similar to those in the TBMD. Pure Au nanowires show the largest Au-Au distances to be somewhere around 3.0–3.1 Å in both cases (this result was independent of the exchange-correlation potential used in the *ab initio* calculations—LDA or GGA—and also was independent of the basis set used—localized or plane wave basis sets). We further study the bonding character of the Au neck atoms, and detail it in terms of the projected DOS, namely, the contribution of each individual neck atom to the electronic structure. In particular, we show how the number of nearest neighbors influences the behavior of the electronic states for each one of these atoms, and how this changes as the wire is stretched. We believe that the results presented here will be useful in the analysis of experiments on Au (and other metallic) nanowires.

Finally, as already mentioned above, the fact that the pure wires always break with a maximum Au-Au distance on the order of 3.0–3.1 Å leaves as an open question the cause of the large Au distances ($\simeq 3.6$ Å) observed experimentally. As we pointed out in Sec. I, these large distances have been attributed to light atoms impurities that are (unintentionally) inserted in between two Au neck atoms. We recently[17] studied the effect of a variety of impurities (namely, H, B, C, N, O, and S) in the rupture of Au NWs, using an *ab initio* procedure similar to the one described here, and we have shown that H seems to be the best candidate to explain the observed distances in the range of 3.6 Å. However, a more extensive and detailed study, where properties beyond interatomic distances are investigated, such as the effect of these impurities in the electronic structure (e.g., projected DOS), would also be of great importance to better understand the properties of NWs. Such a study is currently underway, and we expect to report about it in the near future.

ACKNOWLEDGMENTS

The TBMD code was developed by Florian Kirchhoff as part of the Computational Chemistry and Materials Science Computational Technology Area (CCM CTA)'s contribution to the U.S. Department of Defense CHSSI program. The simulations were performed at the National Center for High Performance Computing in São Paulo (CENAPAD). We acknowledge support from FAPESP. Partial support was provided to E.Z.S., A.J.R.S., and A.F. by CNPq. F.D.N acknowledges support from CNPq. We would also like to acknowledge fruitful discussions with D. Ugarte and V. Rodrigues.

*Email address: zacarias@ifi.unicamp.br
†Email address: ajrsilva@if.usp.br
‡Email address: fazzio@if.usp.br

[1] R. Wiesendanger, *Scanning Probe Microscopy and Spectroscopy* (Cambridge University Press, Cambridge, 1994).
[2] E. Tosatti, S. Prestipino, S. Kostlmeier, A. Dal Corso, and F.D. Di Tolla, Science **291**, 288 (2001).
[3] *Nanowires*, edited by P.A. Serena and N. Garcia (Kluwer, Dordrecht, 1997), Vol. 340.
[4] J.K. Gimzewski and R. Moller, Physica C **38**, 1284 (1987).
[5] R.A. Webb, S. Washburn, C.P. Umbach, and R.B. Laibowitz, Phys. Rev. Lett. **54**, 2696 (1985).
[6] N. Agrait, J.G. Rodrigo, and S. Vieira, Phys. Rev. B **47**, 12 345 (1993).
[7] H. Ohnishi, Y. Kondo, and K. Takayanagi, Nature (London) **395**, 780 (1998).
[8] A.I. Yanson *et al.*, Nature (London) **395**, 783 (1998).
[9] J. Moreland and J.W. Ekin, Physica C **191**, 485 (1992).
[10] C.J. Muller, J.M. Ruitenbeek, and L.J. Jong, Phys. Rev. Lett. **69**, 140 (1992).
[11] Y. Kondo and K. Takayanagi, Phys. Rev. Lett. **79**, 3455 (1997).
[12] Y. Kondo and K. Takayanagi, Science **289**, 606 (2000).
[13] V. Rodrigues, T. Fuhrer, and D. Ugarte, Phys. Rev. Lett. **85**, 4124 (2000).
[14] V. Rodrigues and D. Ugarte, Phys. Rev. B **63**, 073405 (2001).
[15] S.B. Legoas, D.S. Galvão, V. Rodrigues, and D. Ugarte, Phys. Rev. Lett. **88**, 076105 (2002).

[16] S.R. Bahn, N. Lopez, J.K. Norskov, and K.W. Jacobsen, Phys. Rev. B **66**, 081405 (2002).
[17] F.D. Novaes, E.Z. da Silva, A.J.R. da Silva, and A. Fazzio, Phys. Rev. Lett. **90**, 036101 (2003).
[18] N.V. Skorodumova and S.I. Simak, Phys. Rev. B **67**, 121404 (2003).
[19] O. Gulseren, F. Ercolessi, and E. Tosatti, Phys. Rev. Lett. **80**, 3775 (1998).
[20] H. Park, J. Park, A.K.L. Lin, E.H. Anderson, A.P. Alivisatos, and P.L. McEuen, Nature (London) **407**, 57 (2000).
[21] J. Reichert, R. Ochs, D. Beckmann, H.B. Weber, M. Weber, M. Mayor, and H.V. Lohneysen, Phys. Rev. Lett. **88**, 176804 (2002).
[22] H. Hakknen, R. Bernett, and U. Landman, J. Phys. Chem. B **103**, 8814 (1999).
[23] J. Heurich, J.C. Cuevas, W. Wenzel, and G. Schon, Phys. Rev. Lett. **88**, 256803 (2002).
[24] D. Kruger, H. Fucks, R. Rousseau, D. Markx, and M. Parrinello, Phys. Rev. Lett. **89**, 186402 (2002).
[25] U. Landman, W. Luedtke, and N. Burnham, and R.J. Colton, Science **248**, 454 (1990).
[26] E.Z. da Silva, A.J.R. da Silva, and A. Fazzio, Phys. Rev. Lett. **87**, 256102 (2001).
[27] M. Brandbyge *et al.*, Phys. Rev. B **52**, 8499 (1995).
[28] M.J. Mehl and D.A. Papaconstantopoulos, Phys. Rev. B **54**, 4519 (1996).
[29] The NRL TB parameters are available on the World Wide Web at http://cst-www.nrl.navy.mil/bind.
[30] The NRL TB-MD software is available on the World Wide Web at http://cst-www.nrl.navy.mil/bind/dodtb.
[31] F. Kirchhoff, M.J. Mehl, N.I. Papanicolaou, D.A. Papaconstantopoulos, and F.S. Khan, Phys. Rev. B **63**, 195101 (2001).
[32] E.Z. da Silva, A.J.R. da Silva, and A. Fazzio, Comput. Mat. Sci. (to be published).
[33] G. Rubio-Bollinger, S.R. Bahn, N. Agrait, K.W. Jacobsen, and S. Vieira, Phys. Rev. Lett. **87**, 026101 (2001).
[34] P. Hohenberg and W. Kohn, Phys. Rev. **136**, 864B (1964); W. Kohn and L.J. Sham, *ibid.* **140**, 1133A (1965).
[35] P. Ordejón, E. Artacho, and J.M. Soler, Phys. Rev. B **53**, 10 441 (1996); D. Sánchez-Portal, P. Ordejón, E. Artacho, and J.M. Soler, Int. J. Quantum Chem. **65**, 453 (1997).
[36] N. Troullier and J.L. Martins, Phys. Rev. B **43**, 1993 (1991).
[37] H.J. Monkhorst and J.D. Pack, Phys. Rev. B **13**, 5188 (1976). For the pure gold nanowire, the Au-Au maximum distance changed by less than 0.03 Å when the number of **k** points was changed from 1 to 8.
[38] E. Artacho, D. Sánchez-Portal, P. Ordejón, A. Garcia, and J.M. Soler, Phys. Status Solidi B **215**, 809 (1999).
[39] J. Perdew, K. Burke, and M. Ernzerhof, Phys. Rev. Lett. **77**, 3865 (1996).
[40] S. Iijima, Nature (London) **354**, 56 (1991).
[41] Y. Oshima *et al.*, Phys. Rev. B **65**, 121401 (2002).
[42] J.A. Torres *et al.*, Surf. Sci. Lett. **83**, 441 (1999).
[43] Y. Takai, T. Kadwasaki, Y. Kimura, T. Ikuta, and R. Shimizu, Phys. Rev. Lett. **87**, 106105 (2001).
[44] D. Sánchez-Portal, E. Artacho, P. Ordejón, A. Garcia, and J.M. Soler, Phys. Rev. Lett. **83**, 3884 (1999).
[45] B. Hammer, L.B. Hansen, and J.K. Norskov, Phys. Rev. B **59**, 7413 (1999).
[46] F.J. Ribeiro and M.L. Cohen, Phys. Rev. B **68**, 035423 (2003).
[47] J.P. Perdew and Y. Wang, Phys. Rev. B **45**, 13 244 (1992).
[48] D. Vanderbilt, Phys. Rev. B **41**, 7892 (1990).
[49] G. Kresse and J. Hafner, Phys. Rev. B **47**, R558 (1993); G. Kresse and J. Furthmüller, *ibid.* **54**, 11 169 (1996).